A Timoshenko Beam Finite Element Formulation for Thin-Walled Box Girder Considering Inelastic Buckling

S. Li
Department of Naval Architecture, Ocean and Marine Engineering, University of Strathclyde, Glasgow, UK

S. Benson & R.S. Dow
Marine, Offshore and Subsea Technology Group, School of Engineering, Newcastle University, UK

ABSTRACT: A Timoshenko beam finite element model is formulated based on the Lagrange and Hermitian interpolations, in which the transverse shear deformation is explicitly evaluated. To account for the local inelastic buckling, the finite element formulation is coupled with a Smith-type progressive collapse method where the nonlinear responses of local structural members can be assessed. The effect of shear lag is accounted by an effective breadth theory. This coupled model enables an efficient prediction of the flexural behaviour of a thin-walled box girder under lateral loading. To demonstrate its capability, a case study is completed on a single-skin box girder under four-point bending. Equivalent finite shell element analysis is carried out for validation. The proposed method shows a close correlation with the shell element model in both strength and stiffness predictions. It is found that the effect of shear lag is significant in this case study, which substantially reduces the stiffness of the box girder.

1 INTRODUCTION

A simplified progressive collapse method (Smith method), which is the codified approach in contemporary ship structural design guideline such as the IACS Common Structural Rule (CSR), can be adopted for the ultimate strength analysis of ship hull girders. Since the original development by Smith (1977), the advancements to this simplified progressive collapse method includes different formulations (Gordo and Guedes Soares, 1996), extensions for biaxial bending (Smith and Dow, 1986), torsion (Syrigou et al., 2018), multi-frame collapse (Benson et al., 2013), cyclic load (Li et al., 2020), local bottom pressure (Tasumi et al., 2020) and applications for damaged ships (Fujikubo et al., 2012; Li et al., 2019). The principle algorithm of Smith-type method is well-established and consistent, relying on the evaluation of local component's tangent stiffness through a load-shortening curve. Many methods are available to predict the load-shortening response of structural elements (Dow and Smith, 1986; Yao and Nikolov, 1991; Yao and Nikolov, 1992; Gordo and Guedes Soares, 1993; Benson et al., 2015; Li et al., 2019; Li et al., 2020) and because of which a large uncertainty can be induced. Deterministic studies on the uncertainty due to structural member's response were presented by ISSC (2000) and Li et al. (2020). A probabilistic approach to evaluate the computational uncertainty of Smith method was introduced by Li et al. (2021).

However, even with a substantial development, the simplified progressive collapse method is still limited to the prediction of ship hull girder behaviour characterized by the cross sectional bending moment versus curvature relationship. A direct analysis for the responses to the lateral distributed loads (i.e. weight, buoyancy and dynamic wave pressure) cannot be completed, which limits the coupling of this method with a hydrodynamic methodology. This issue can be resolved by combining the simplified progressive collapse method with a finite beam element formulation, as originally proposed by Tanaka et al. (2015). The approach was further extended by Ko et al. (2018) to develop a hydro-elastoplastic approach. In these pioneering works, an Euler-Bernoulli beam finite element was formulated. Whist this is an efficient and reasonable approach, the Timoshenko beam formulation could be a better representation of ship-type thin-walled box girders in terms of the global bending stiffness prediction. As the major application of this method is to support the development of a coupled dynamic analysis method considering fluid-structure interaction, an accurate prediction of the bending stiffness is highly important.

Thus, extended upon the previous works by Tanaka et al. (2015) and Ko et al. (2018), a method is outlined in this paper to predict the global flexural response of thin-walled box girders considering the local inelastic buckling. A Timoshenko beam finite element method (FEM) is combined with simplified progressive collapse method (Smith method). The

former enables the simulation of the global behaviour of a hull girder, while the latter provides an efficient evaluation of the structural nonlinearity due to local inelastic buckling failure. The effect of shear lag at the flanges is taken into account by an effective breadth theory. The proposed methodology is detailed in Section 2 introducing the derivation of beam element stiffness matrix based on Lagrange/Hermitian interpolations and the coupling between FEM and Smith method. A validation is completed in Section 3 by a comparison with the nonlinear finite shell element analysis for a ship-type thin-walled box girder in four-point bending. Conclusions are summarized in Section 4.

2 METHODOLOGY

2.1 Principle

The proposed methodology is illustrated by the flowchart in Figure 1, highlighting the key steps in Timoshenko beam FEM, Smith method and their coupling. A ship hull girder is discretized longitudinally into beam elements. The cross section of each beam element is subdivided into plate-stiffener combination structural segments. A load-shortening curve is assigned to each structural segments to characterize its response to the in-plane compression and tension. With these load-shortening curves, the tangent stiffness of structural segments and the instantaneous neutral axis of the cross section can be evaluated. These are then input to calculate the stiffness matrix of each beam element with an independency assumption that there is no interaction between each structural segment. In the assembling of global stiffness matrix, an effective breadth concept is employed to evaluate the shear lag effect at the flanges of the thin-walled model. The global force-displacement equation of the finite element model is solved incrementally by a displacement-controlled technique. The incremental displacement vector is utilized in combination with the strain-nodal displacement relationship (i.e. **B**) to estimate the strain increment of each structural segments in the beam element. The updates of structural segment's tangent stiffness and the neutral axis of the beam element cross section are driven by these incremental strain estimations, which is the key step in the coupling between Timoshenko beam FEM and the Smith method.

2.2 Timoshenko Beam

As shown in Figure 2, a Timoshenko beam finite element with four degrees of freedom at each node is considered, including axial displacement u, vertical displacement w, vertical rotation θ and shear ψ, which correspond to the axial force F_x, the vertical force F_z that purely induces vertical displacement , the vertical bending moment M_y and the shear force Q. The vertical displacment, vertical rotation and the shear are related by Equation (1), which is also illustrated by Figure 3. For a two-node Timoshenko beam finite element, the governing equation is given by Equation (2) where $\mathbf{F^e}$ is the nodal force vector, $\boldsymbol{\delta}^{\mathbf{e}}$ is the nodal displacement vector and **K** is the element stiffness matrix.

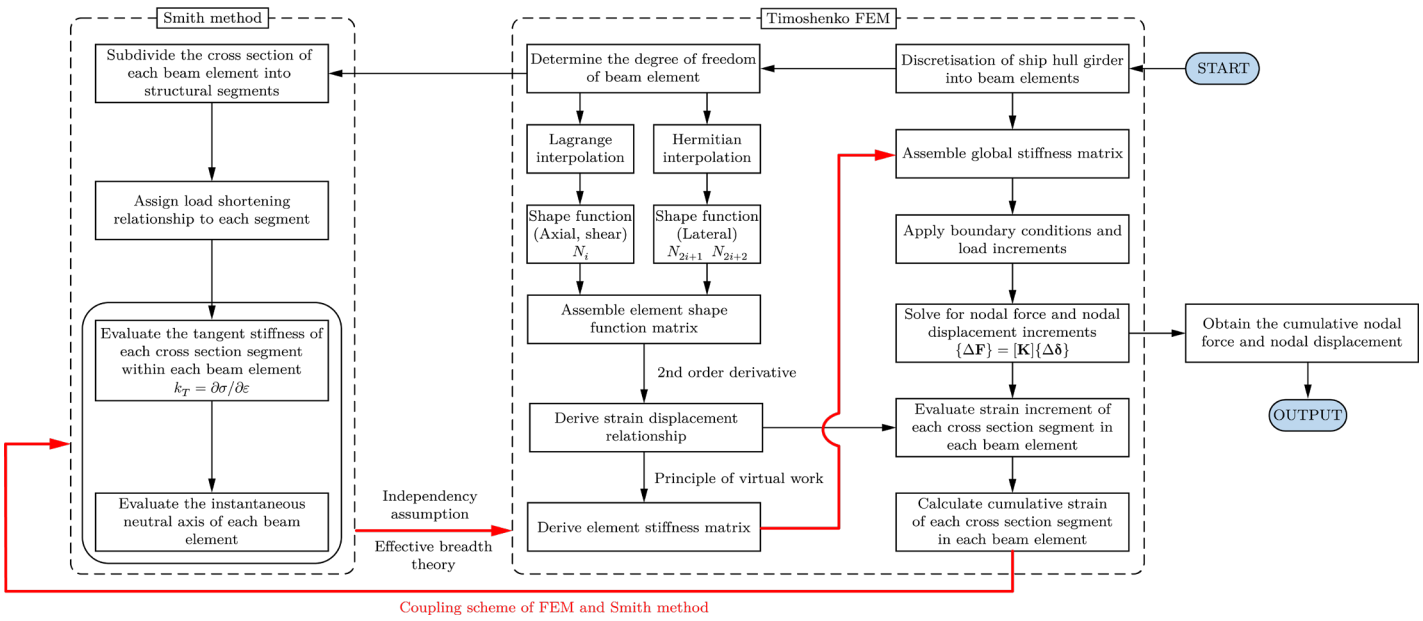

Figure 1. Flowchart of the proposed method

$$\theta = \frac{dw}{dx} + \psi \tag{1}$$

$$\mathbf{F^e} = \mathbf{K} \cdot \boldsymbol{\delta}^{\mathbf{e}} \tag{2}$$

where

$$\mathbf{F^e} = \{F_{x1} \quad F_{z1} \quad M_{y1} \quad Q_1 \quad F_{x2} \quad F_{z2} \quad M_{y2} \quad Q_2\}^T$$

$$\boldsymbol{\delta}^{\mathbf{e}} = \{u_1 \quad w_2 \quad \theta_1 \quad \psi_1 \quad u_2 \quad w_2 \quad \theta_2 \quad \psi_2\}^T$$

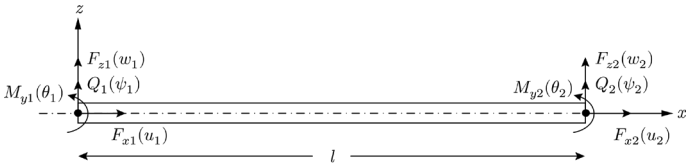

Figure 2. Timoshenko beam finite element with four degrees of freedom at each node

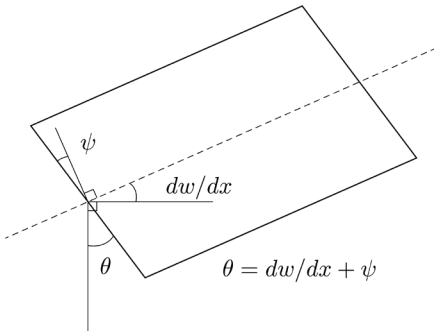

Figure 3. Relationship between the vertical displacement, the vertical rotation and the shear in the Timoshenko beam

The element stiffness is derived with the following assumptions in accordance with Thomas et al. (1973):

- Deformation is limited to bending in the direction of a principle axis;
- Cross section is symmetric about both principle axes;
- The axis of the beam is straight.

The displacement field within the element is related to the nodal displacement via shape functions, given as:

$$\boldsymbol{\delta} = \{u(x) \quad w(x) \quad \theta(x) \quad \psi(x)\}^T = \mathbf{N} \cdot \boldsymbol{\delta}^{\mathbf{e}} \tag{3}$$

The conventional derivation usually starts from assuming a n-termed polynomial with unknown coefficients where n is the total degrees of freedom. This approach requires considerable manual calculations. The alternative procedure using Lagrange and Hermitian interpolation as presented in the following provides a systematic approach to allow a simpler computer code development (Augarde, 1998). The shape functions related to the axial displacement and shear, e.g. N_1 and N_2, can be derived by Lagrange interpolation. The shape functions related to the bending displacement, e.g. N_3, N_4, N_5 and N_6, can be derived by Hermitian interpolation. However, the shape functions corresponding to the rotational displacement exclude the effect of transverse shear deformation. To account for shear deformation ψ, the interactive terms between the rotational displacement and the shear are modified in accordance with Equation (1). Hence, the general expression of shape function matrix can be written as follows:

$$\mathbf{N} = [\mathbf{N_1} \quad \mathbf{N_2}] \tag{4}$$

where

$$\mathbf{N_1} = \begin{bmatrix} N_1 & 0 & 0 & 0 \\ 0 & N_3 & N_4 & -N_4 \\ 0 & dN_3/dx & dN_4/dx & -dN_4/dx + N_1 \\ 0 & 0 & 0 & N_1 \end{bmatrix}$$

$$\mathbf{N_2} = \begin{bmatrix} N_2 & 0 & 0 & 0 \\ 0 & N_5 & N_6 & -N_6 \\ 0 & dN_5/dx & dN_6/dx & -dN_6/dx + N_2 \\ 0 & 0 & 0 & N_2 \end{bmatrix}$$

Based on Lagrange interpolation, the shape function N_1 and N_2 are derived by the following equations.

$$N_i(\xi) = \prod_{j=1, j\neq i}^{m} \frac{\xi - \xi_j}{\xi_i - \xi_j} \tag{5}$$

$$\xi = x/l \tag{6}$$

Hence, the following can be obtained:

$$N_1 = \frac{\xi - \xi_2}{\xi_1 - \xi_2} = \frac{\xi - 1}{0 - 1} = 1 - \xi \tag{7}$$

$$N_2 = \frac{\xi - \xi_1}{\xi_2 - \xi_1} = \frac{\xi - 0}{1 - 0} = \xi \tag{8}$$

Based on Hermitian interpolation, the vertical deflection field of a two-node beam element with an overall length of l can be expressed as follows:

$$w(x) = \sum_{i=1}^{m} \left[H_{0i}^r w_i + H_{1i}^r \left(\frac{dw}{dx}\right)_i + \cdots + H_{ji}^r \left(\frac{d^r w}{dx^r}\right)_i \right] \tag{8}$$

where

H_{ji}^r = Hermite polynomial of level r, relating to node i and to derivative order j of $w(x)$

m = Number of nodes

r = The level of Hermite polynomial, indicating the highest order derivative used in the interpolation

The shape functions of beam elements are the level-one Hermitian polynomials, i.e. $r = 1$. The level-one Hermitian polynomials can be derived from the Lagrange polynomials by the following formulae:

$$H_{0i}^r = [1 - 2l(\xi - \xi_i)L_i'(\xi_i)][L_i(\xi)]^2 \quad (9)$$

$$H_{1i}^r = l(\xi - \xi_i)[L_i(\xi)]^2 \quad (10)$$

where

$$L_i(\xi) = \prod_{j=1, j\neq i}^{m} \frac{\xi - \xi_j}{\xi_i - \xi_j}$$

Following Equation (9) and (10), the Lagrange polynomials and their derivatives are derived as follows.

$$L_1(\xi) = \frac{\xi - \xi_2}{\xi_1 - \xi_2} = \frac{\xi - 1}{0 - 1} = 1 - \xi \quad (11)$$

$$L_2(\xi) = \frac{\xi - \xi_1}{\xi_2 - \xi_1} = \frac{\xi - 0}{1 - 0} = \xi \quad (12)$$

$$L_1'(\xi) = -1/l \quad (13)$$

$$L_2'(\xi) = 1/l \quad (14)$$

Substituting Equation (11) to (14) into Equation (9) and (10), the Hermitian polynomials are given as:

$$H_{01}^r = [1 - 2l(\xi - \xi_1)L_1'(\xi_1)][L_1(\xi)]^2$$
$$= 1 - 3\xi^2 + 2\xi^3 \quad (15)$$

$$H_{11}^r = l(\xi - \xi_1)[L_1(\xi)]^2$$
$$= x(1 - \xi)^2 \quad (16)$$

$$H_{02}^r = [1 - 2l(\xi - \xi_2)L_2'(\xi_2)][L_2(\xi)]^2$$
$$= 3\xi^2 - 2\xi^3 \quad (17)$$

$$H_{12}^r = l(\xi - \xi_2)[L_2(\xi)]^2$$
$$= x(\xi^2 - \xi) \quad (18)$$

Since $N_3 = H_{01}^r, N_4 = H_{11}^r, N_5 = H_{02}^r$ and $N_6 = H_{12}^r$, the shape function matrix of a two-node Timoshenko beam element (Equation 4) can be derived. Based on beam theory, the axial strain due to axial force ε_x^a, axial strain due to bending ε_x^b and the transverse shear strain γ_{xy} are given by the following:

$$\varepsilon_x^a \approx \frac{du}{dx} \quad (19)$$

$$\varepsilon_x^b \approx -z\frac{d\theta}{dx} \quad (20)$$

$$\gamma_{xy} \approx \psi \quad (21)$$

Hence, by substituting Equation (19), (20) and (21) into shape function matrix (Equation 4), a strain-nodal displacement relationship can be obtained.

$$\boldsymbol{\varepsilon} = \{\varepsilon_x^a \quad \varepsilon_x^b \quad \gamma_{xy}\}^T = \mathbf{B} \cdot \boldsymbol{\delta}^{\mathbf{e}} \quad (21)$$

where

$$\mathbf{B} = [\mathbf{B_1} \quad \mathbf{B_2}] \quad (22)$$

$$\mathbf{B_1} = \begin{bmatrix} \frac{-1}{l} & 0 & 0 & 0 \\ 0 & z\left(\frac{6}{l^2} - \frac{12x}{l^3}\right) & z\left(\frac{4}{l} - \frac{6x}{l^2}\right) & z\left(\frac{-3}{l} + \frac{6x}{l^2}\right) \\ 0 & 0 & 0 & 1 - \frac{x}{l} \end{bmatrix}$$

$$\mathbf{B_2} = \begin{bmatrix} \frac{1}{l} & 0 & 0 & 0 \\ 0 & z\left(\frac{-6}{l^2} + \frac{12x}{l^3}\right) & z\left(\frac{2}{l} - \frac{6x}{l^2}\right) & z\left(\frac{-3}{l} + \frac{6x}{l^2}\right) \\ 0 & 0 & 0 & \frac{x}{l} \end{bmatrix}$$

Following the elastic properties of the element, the relationship between the internal stresses and the strain can be given as follows.

$$\boldsymbol{\sigma} = \mathbf{D} \cdot \boldsymbol{\varepsilon} = \mathbf{D} \cdot \mathbf{B} \cdot \boldsymbol{\delta}^{\mathbf{e}} \quad (23)$$

where

$$\boldsymbol{\sigma} = \{\sigma_x^a \quad \sigma_x^b \quad \tau\}^T$$

$$\mathbf{D} = \begin{bmatrix} E & 0 & 0 \\ 0 & E & 0 \\ 0 & 0 & G \end{bmatrix}$$

The element stiffness matrix is derived using the principle of virtual work. It is stated that during any virtual displacement imposed on the element, the total external work done by the nodal loads must equal to the total internal work done by the stresses. Let $\boldsymbol{\delta}^{*\mathbf{e}}$ be the vector of virtual nodal displacement, the external work done by the nodal loads can be expressed as:

$$W_{ext} = \boldsymbol{\delta}^{*\mathbf{e}T} \cdot \mathbf{F}^{\mathbf{e}} \quad (24)$$

Since the virtual displacements cause virtual strain $\boldsymbol{\varepsilon}^*$ within the element where the actual stresses are $\boldsymbol{\sigma}$, the internal work is given by:

$$W_{int} = \iiint \boldsymbol{\varepsilon}^{*T} \cdot \boldsymbol{\sigma}\, dxdydz \quad (25)$$

Applying the virtual nodal displacement yields:

$$\boldsymbol{\varepsilon}^{*\mathbf{T}} = \mathbf{B} \cdot \boldsymbol{\delta}^{*\mathbf{e}} \quad (26)$$

Substituting Equation (23) and (26) into Equation (25) gives

$$W_{int} = \boldsymbol{\delta}^{*\mathbf{e}T} \iiint \mathbf{B}^T \cdot \mathbf{D} \cdot \mathbf{B}\; dxdydz\, \boldsymbol{\delta}^{\mathbf{e}} \quad (27)$$

Equating the external and internal work and setting the virtual nodal displacement to unity value gives:

$$\mathbf{F^e} = \iiint \mathbf{B^T} \cdot \mathbf{D} \cdot \mathbf{B}\ dxdydz\ \boldsymbol{\delta^e} \tag{28}$$

By examining Equation (28) with reference to Equation (2), it is easy to observe that the stiffness matrix can be obtained by

$$\mathbf{K} = \iiint \mathbf{B^T} \cdot \mathbf{D} \cdot \mathbf{B}\ dxdydz \tag{29}$$

2.3 Coupling between Timoshenko Beam Finite element and Smith Method

Smith-type progressive collapse method is originally introduced to predict the bending moment versus curvature relationship of a ship hull girder. The cross section of a ship hull girder is subdivided into structural segments. A load-shortening curve is assigned to each structural segment, which describes its response to the in-plane compression and tension. The tangent stiffness k_T^i of each segment is numerically evaluated from the load-shortening curve by a central difference technique as given by Equation (30). The adequacy of this tangent stiffness evaluation can be ensured by defining the load-shortening curve with a suffcient number of data points. The instantaneous neutral axis of the cross section is calculated by Equation (31), which is essentially the first moment of area of the cross section accounting for the effectiveness loss due to local buckling. The segment tangent stiffness and the cross seciton neutral axis position are utilised in the original formulation to estimate the bending stiffness of the cross section, which allows for the calculation of bending moment increment for a given incremntal curvature.

$$k_T^i = \partial\sigma/\partial\varepsilon = (\sigma_{x+\Delta x} - \sigma_x)/(\varepsilon_{x+\Delta x} - \varepsilon_x) \tag{30}$$

$$z_{NA} = \left(\sum_{i=1}^{n} z_i k_T^i A_i\right)/\left(\sum_{i=1}^{n} k_T^i A_i\right) \tag{31}$$

Instead of following this original approach, the tangent stiffness (Equation 30) and neutral axis potition (Equation 31) are employed to calculate the stiffness matrix of the Timoshenko beam element. The elastic material property in Equation (23) is replaced with the tangent stiffness, and the instantaneous neutral axis will be employed to calculate the relative coordinate of each elemenet in Equation (22). Thus, in combination with Equation (29), the stiffness matrix of a Timoshenko beam element can be expressed as Equation (32). Besides, it is assumed that the relationship between the shear stiffness and in-plane stiffness is always consistent with the one in the elastic state.

$$\mathbf{K} = \begin{bmatrix} K_1 & & & \cdots & \cdots & & & \mathbf{S} \\ 0 & K_2 & & & & & & \\ 0 & K_3 & K_4 & & & \ddots & & \\ 0 & -K_3 & K_5 & K_7 & & & & \vdots \\ -K_1 & 0 & 0 & 0 & K_1 & & & \vdots \\ 0 & -K_2 & -K_3 & K_3 & 0 & K_2 & & \\ 0 & K_3 & K_6 & K_5 & 0 & -K_3 & K_4 & \\ 0 & -K_3 & K_5 & K_8 & 0 & K_3 & K_5 & K_7 \end{bmatrix} \tag{32}$$

where

$K_1 = \sum_{i=1}^{n} k_T^i A_i \frac{1}{l}$

$K_2 = \sum_{i=1}^{n} k_T^i A_i (z_i - z_{NA})^2 \frac{12}{l^3}$

$K_3 = \sum_{i=1}^{n} k_T^i A_i (z_i - z_{NA})^2 \frac{6}{l^2}$

$K_4 = \sum_{i=1}^{n} k_T^i A_i (z_i - z_{NA})^2 \frac{4}{l}$

$K_5 = \sum_{i=1}^{n} k_T^i A_i (z_i - z_{NA})^2 \frac{-3}{l}$

$K_6 = \sum_{i=1}^{n} k_T^i A_i (z_i - z_{NA})^2 \frac{2}{l}$

$K_7 = \sum_{i=1}^{n} k_T^i A_i (z_i - z_{NA})^2 \frac{3}{l} + \sum_{i=1}^{n} kG_i A_i \frac{l}{3}$

$K_8 = \sum_{i=1}^{n} k_T^i A_i (z_i - z_{NA})^2 \frac{3}{l} + \sum_{i=1}^{n} kG_i A_i \frac{l}{6}$

2.4 Shear Coefficient

The Timoshenko beam is effectively based on a first-order shear deformation theory, which assumes an uniform distribution of the shear deformation. Thus, as appearing in the element stiffness matrix (Equation 32), a shear coefficient k is applied to account for the fact that the shear stress and shear strain are in reality not uniformly distributed over cross section. This coefficient is dependent on the dimension and moreover the shape of the cross section. In this paper, the shear coefficient is calculated following the formula proposed by Cowper (1966). For a thin-walled box girder, this is given as Equation (33) with all parameters defined by Figure 3.

$$k = k_1/(k_2 + k_3 + k_4) \tag{33}$$

where

$k_1 = 10(1+\nu)(1+3m)^2$

$k_2 = (12 + 72m + 150m^2 + 90m^3)$

$k_3 = \nu(11 + 66m + 135m^2 + 90m^3)$

$k_4 = 10n^2[(3+\nu)m + 3m^2]$

$m = bt_1/bt$

$n = b/h$

ν = Poisson's ratio

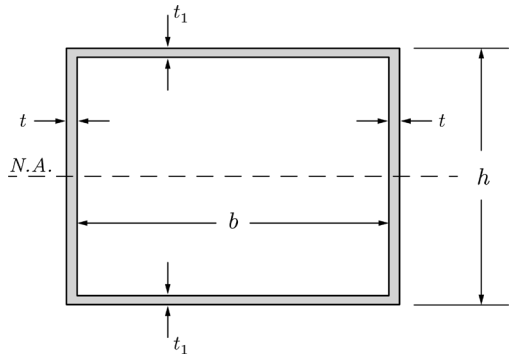

Figure 3. Parameters for calculating the shear coefficient of a thin-walled box girder

2.5 Shear Lag

Beam theories, including Timoshenko and Euler-Bernoulli, assume that the plane cross section remains plane, and therefore the bending stress is directly propotional to the distance from the neutral axis. Thus, in any flange-and-web type of beam, such as a thin-walled ship hull girder, the stress should be constant across the flange. However, when the lateral loads are applied, these loads are absorbed by the webs and not by the flanges. Even the lateral loads initially act on the flange, such as the distributed loads on a ship hull, they are immediately transferred to the webs by the transverse frames. Thus, the lateral loads cause the webs to deflect to some radius of curvature, as in Figure 4 showing a portion of a thin-walled box girder under four-point bending. As discussed by Hughes and Paik (2013), a warping distortion occurs at the flange and therfore the plane cross section do not remain plane. This leads to the inner portion of the flange carries less bending stress and is therefore less effective than the outer portion. In other words, the bending stress remote from a web "lags behind" the stress near the web. This phenomenon is usually termed the shear lag effect.

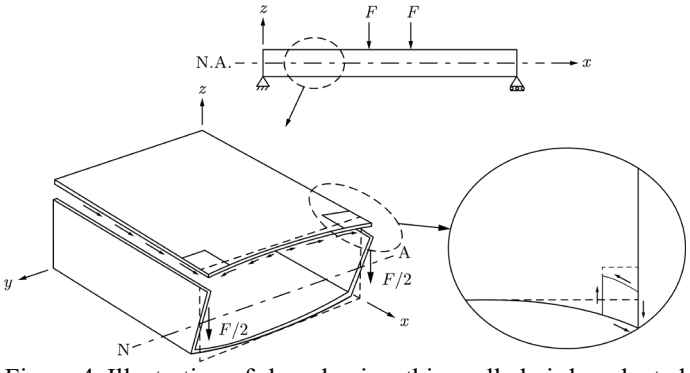

Figure 4. Illustration of shear lag in a thin-walled girder adapted from Hughes and Paik (2013)

To deal with shear lag effect, the effective breadth concept as illustrated by Figure 5 is a practical approach. This should be clearly distinguished with the effective width concept, which is proposed to deal with the plate buckling. In the effective breadth theory, the parabolic stress distribution at the flanges is replaced by two uniform strips with the same magnitude as the maximum stress in the parabolic distribution. Since the longitudinal force at the flange must be in equilibrium, the effective breadth b_e can determined following Equation (34). In this paper, the effective breadth is estimated by performing a linear elastic finite element analysis on the target structure with coarse mesh. The stress distributions at the flanges of the structures are then acquired for calculating the effective breadth.

$$b_e \sigma_{max} = \int_0^b \sigma dy \tag{34}$$

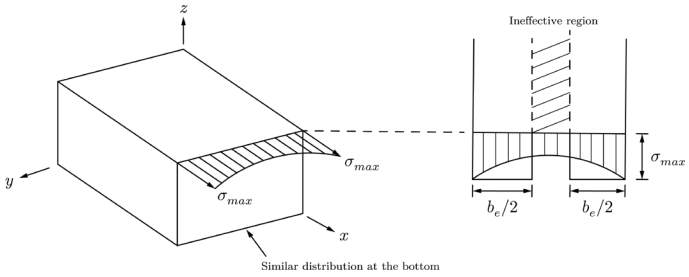

Figure 5. Shear lag stress distribution in flange and effective breadth concept adapted from Hughes and Paik (2013)

3 VALIDATION

3.1 Model Characteristics

The proposed methodology is validated by comparing with the nonlinear finite shell element analysis for a thin-walled box girder in four-point bending. The principal of the model is summarized in Table 1. The cross section of the case study model is shown in Figure 6. It is a simple single-skin box girder, with an overall breadth of 5950mm and overall depth of 4250mm. The whole model consists of 19 sections, each of which has a length of 2550mm and is transversely stiffened by flat-bar frames. The scantling of the transverse frames are properly scaled such that an inter-frame collapse is the dominated failure mode.

Table 1. Principal of the case study model

Overall	L [mm]	B [mm]	D [mm]	
	48450	5950	4250	
Local plating	b [mm]		t_p [mm]	
	850		16	
Long. stiffener	h_w [mm]	t_w[mm]	b_f [mm]	t_f [mm]
	235	10	90	15
Trans. frame	h_w [mm]		t_w [mm]	
	500		20	
Material	σ_Y [MPa]		E [MPa]	
	313.6		205800	

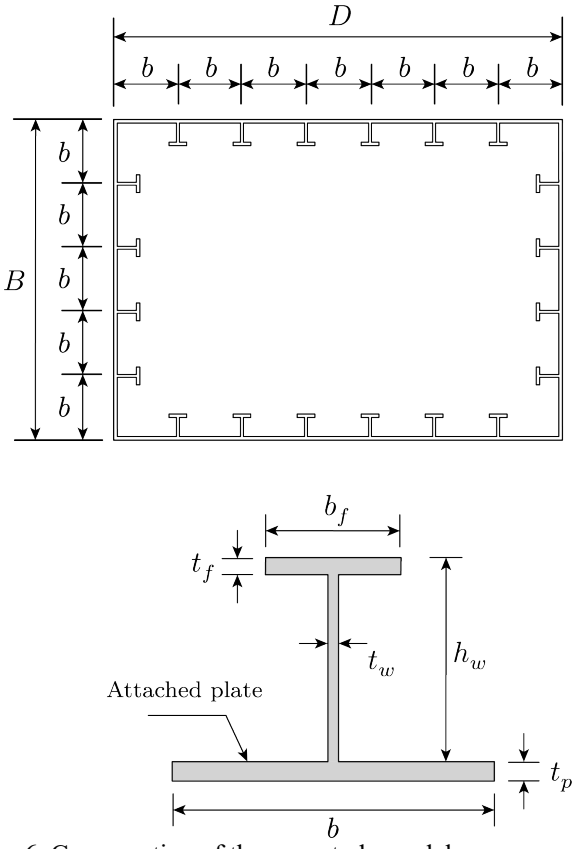

Figure 6. Cross section of the case study model

3.2 Finite Element Modelling

For validation, a numerical model is developed with four-node shell elements and three-node triangular shell elements. As the final collapse involving inelastic buckling is expected to take place at the central part of the model while the others generally remains linear elastic, different mesh densities are applied as shown in Figure 7. The initial imperfection modelling is consistent with the recommendation by ISSC (2012) and Benson et al. (2012).

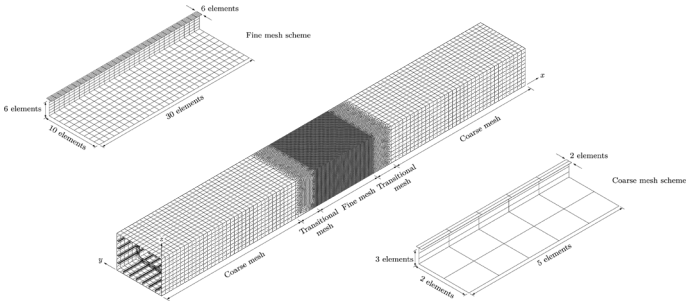

Figure 7. Meshing scheme of the numerical shell model

The boundary condition and loading application are illustrated in Figure 8. Four reference points are created as illustrated, which are coupled with all nodes with the same longitudinal coordinates. For the reference points at the model ends, their vertical coordinates must be consistent with elastic neutral axis of the cross section and longitudinal coordinates must be same with the end cross sections. This is to allow the edge plane to rotate about the neutral axis, which is in line with the beam theory. Displacement-controlled loading application is adopted to enable the prediction of post-collapse behaviour.

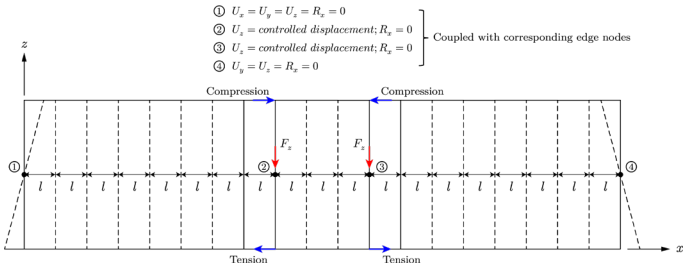

Figure 8. Boundary condition and loading application of the shell model

3.3 Analytical Modelling

In the analytical modelling (Figure 9), the entire box girder is discretised into 11 Timoshenko beam elements. The cross section is subdivided with 28 unstiffened plates and stiffened panel segments considering the inelastic buckling response. Hard corner is not considered and the unstiffened plate segment will follow the same load-shortening behaviour as the adjacent stiffened panel segments. This is based on the observation in preliminary study on shell model. It was found that the intersection between the flanges and webs of the cross section also suffers from significant buckling. Hence, it is not reasonable to define their behaviours as elastic-perfectly plastic.

An adaptable algorithm is adopted to predict the load-shortening curve of structural segments from four characteristics: elastic stiffness, ultimate compressive strength, ultimate strain and post-collapse decay (Li et al., 2020). Displacement-controlled load is applied on nodes 5 and 6. Node 1 is constrained in axial and vertical direction whilst node 12 is constrained only in vertical direction, which is consistent with the shell model boundary conditions.

To account for the effect of shear lag, a linear elastic analysis using shell element model is completed. A coarse mesh consistent with the illustration in Figure 7 is adopted for the entire model.

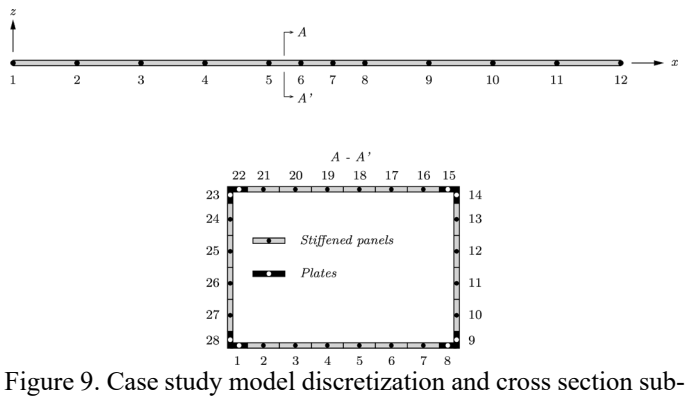

Figure 9. Case study model discretization and cross section subdivision in the analytical modelling

3.4 Results and Discussions

The stress distributions at the flanges obtained from the linear elastic analysis is shown in Figure 10. The distributions of the central three bays are not shown, as they are subjected to a pure bending moment. In all sections the stress distributions show a parabolic pattern, implying that the shear lag occurs due to the shear force. The section near the boundary has the largest influence of shear lag, in which the resultant stress at the central flange deviates the most with that at the intersections with the webs. The effective breadth calculated in accordance with Equation (34) is also shown in Figure 10. These are applied in the flanges of all sections under shear force, i.e. excluding the central three bays. A reduced cross sectional area is thus applied when evaluating the beam element stiffness matrix.

The comparison of the force-displacement diagrams predicted by the analytical method and the finite shell element model is shown in Figure 11(a), which can be interpreted in combination with the neutral axis translation traced in Figure 11(b). The collapse of this case study model is initiated by the onset of buckling of the deck panels, which leads to a substantial vertical displacement of the neutral axis toward the bottom. This is followed by the onset of buckling of the upper side shell panels, immediate to which the buckling collapse of the deck panel occurs. Soon after this local failure, the overall collapse of the entire cross section takes place. The global deflections of the case study models at four critical instances are shown in Figure 11(c). The overall deflection modes in all cases are of a single sinusoidal half-wave, with an increasing magnitude during the progressive collapse. All of these comparisons demonstrates that the accuracy of the proposed analytical method is acceptable in terms of predicting the global flexural behaviour and the ultimate collapse strength.

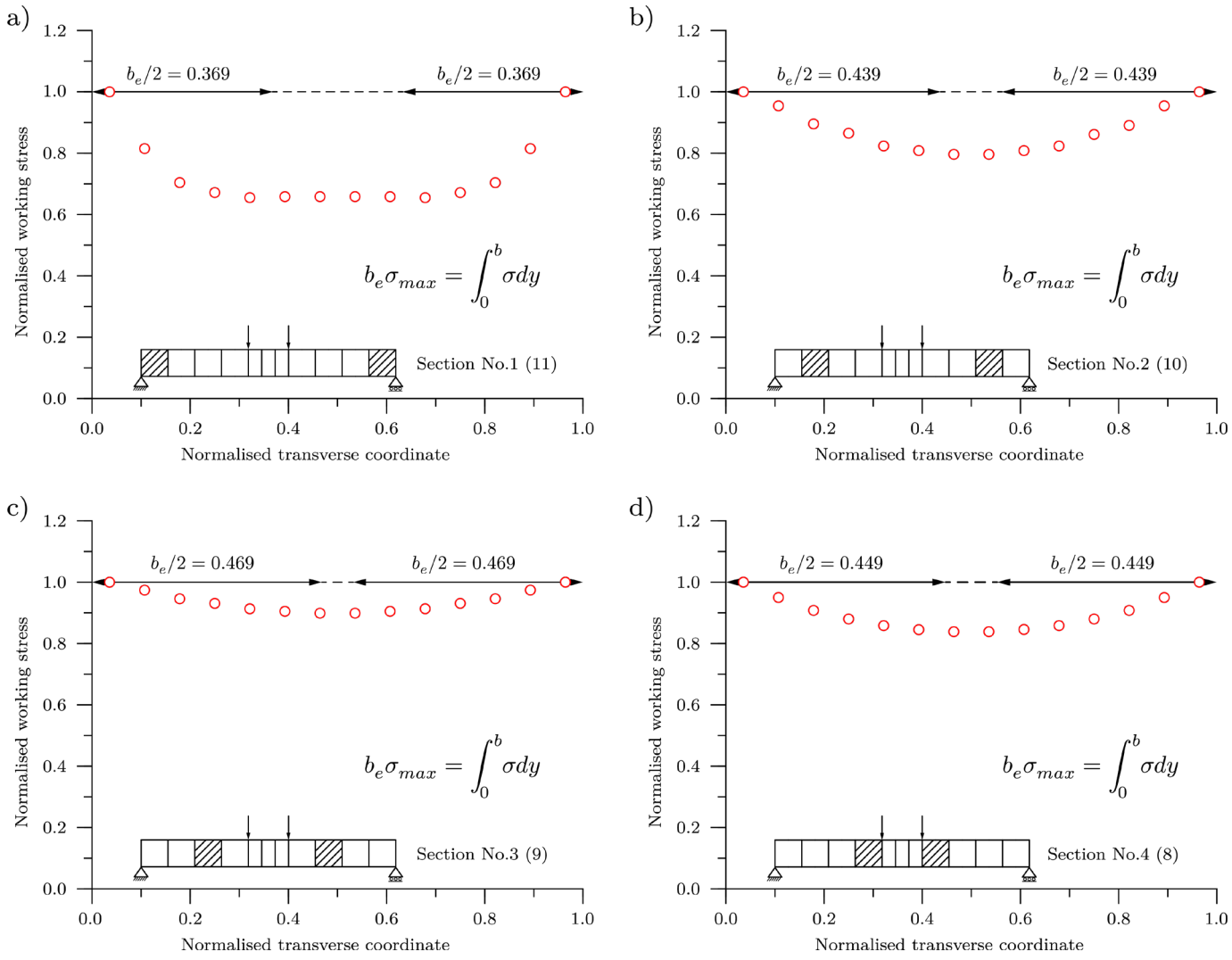

Figure 10. Shear lag stress distributions at the model flanges

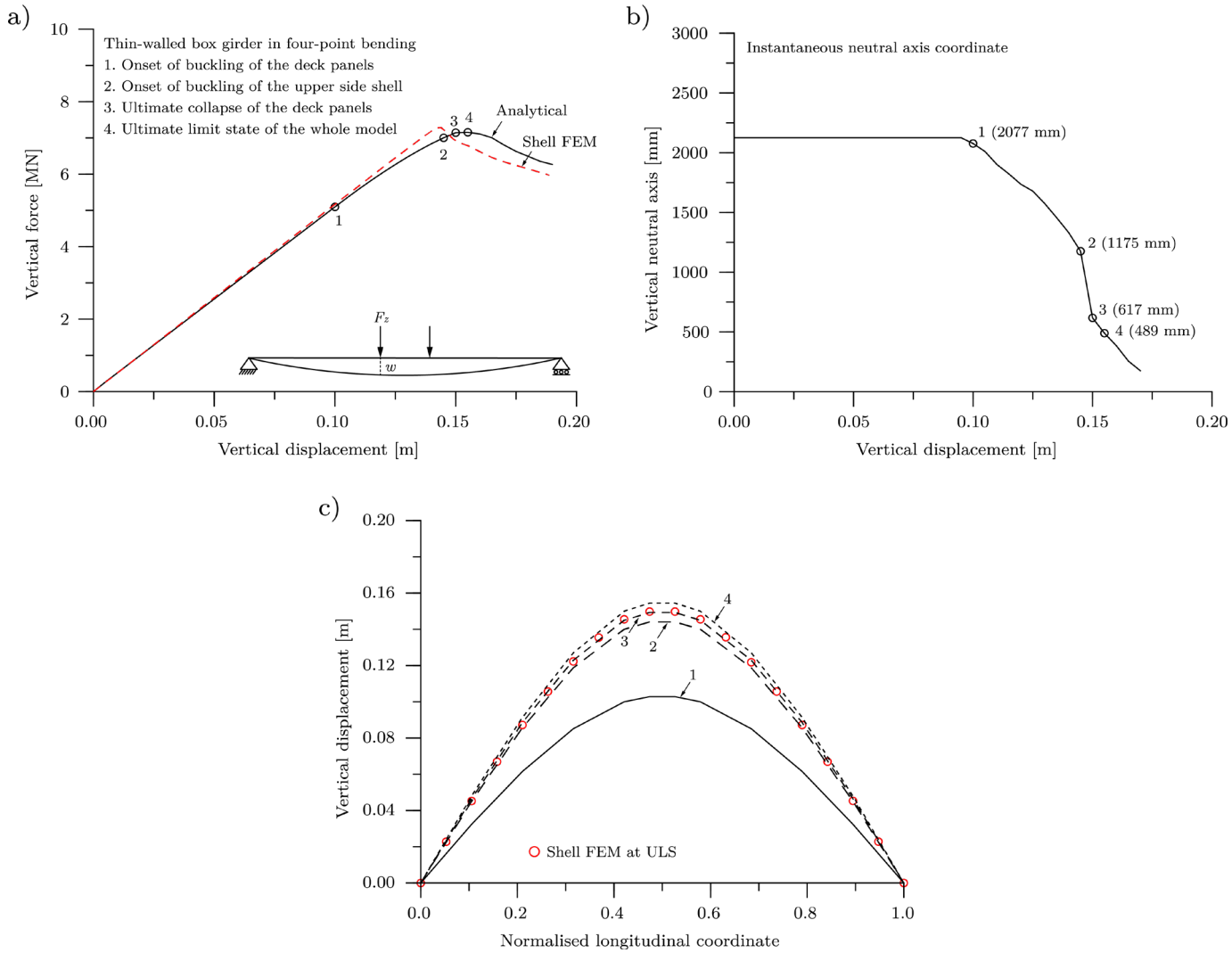

Figure 11. a) Force-displacement diagram; b) Translation of neutral axis; c) Global deflection

4 CONCLUSIONS

A novel analytical method is introduced in this paper by coupling the Timoshenko beam finite element with the Smith-type progressive collapse method. With this approach, the global flexural response of a thin-walled box girder considering the local inelastic buckling can be predicted. From this work, the following conclusions may be drawn:

- It is feasible to combined a finite beam element with the Smith-type progressive collapse method, such that the capability of the latter can be extended to simulate the global flexural response of thin-walled box girder structures.
- The proposed coupled method provides an accurate prediction of the strength and stiffness of a thin-walled box girder under lateral loads, as demonstrated by the validation with the shell model.
- Shear lag might be a critical phenomenon, which significantly affects flexural stiffness of the box girder. To account for the effects of shear lag, the effective breadth concept can be employed. A simple linear elastic analysis based on a finite shell element model with coarse mesh is able to provide the stress distributions at the flanges, which are sufficient to evaluate the effective breadth.

REFERENCES

Augarde, C.E., 1998. Generation of shape functions for straight beam elements. Computers and Structures, 68, 555-560.

Benson S, Downes J, Dow RS. 2015. Overall buckling of lightweight stiffened panels using an adapted orthotropic plate method. Engineering Structures, 85, 107–117.

Benson, S., Downes, J., Dow, R.S., 2013. Compartment level progressive collapse analysis of lightweight ship structures. Marine Structures 31, 44–62.

Benson, S., Downes, J., Dow, R.S., 2012. An automated finite element methodology for hull girder progressive collapse analysis. In: 13th International Marine Design Conference, Glasgow, Scotland.

Cowper, G.R., 1966. The shear coefficient in Timoshenko's beam theory. Journal of Applied Mechanics, 33, 335-340.

Dow, R.S., Smith, C.S.. 1986. FABSTRAN: A computer program for frame and beam static and transient response analysis (Nonlinear). ARE report TR86205.

Fujikubo, M., Zubair Muis Alie, M., Takemura, K., Iijima, K., Oka, S., 2012. Residual hull girder strength of asymmetrically damaged ships. Journal of Japan Society of Naval Architects and Ocean Engineers, 16, 131-140.

Gordo, J.M., Guedes Soares, C., 1996. Approximate method to evaluate the hull girder collapse strength. Marine Structures, 9, 449–470.

Gordo JM, Guedes Soares C. 1993. Approximate load-shortening curves for stiffened plates under uniaxial compression. In Proceeding: Integrity of Offshore Structures 5.

Hughes, O.F., Paik, J.K., 2013. Ship Structural Analysis and Design. The Society of Naval Architects and Marine Engineers, New Jersey, USA.

ISSC. 2000. Ultimate Strength Report. Nagasaki, Japan.

ISSC. 2012. Ultimate Strength Report. Rostock, Germany.

Ko H., Tatsumi, A., Iijima, K., Fujikubo, M., 2018. Collapse analysis of ship hull girder using hydro-elastoplastic beam model. In: Proceedings of the 37th International Conference on Ocean, Offshore & Arctic Engineering (OMAE), Madrid, Spain.

Li, S., Hu, Z., & Benson, S., 2020. Progressive collapse analysis of ship hull girders subjected to extreme cyclic bending. Marine Structures, 73, 102803.

Li, S., Hu, Z., Benson, S., 2019. Bending response of a damaged ship hull girder predicted by the cyclic progressive collapse method. In Proceeding: 8th International Conference on Collision and Grounding of Ships and Offshore Structures, Lisbon, Portugal.

Li, S., Hu, Z., Benson, S., 2020. Ultimate strength performance of a damaged container ship. In Proceeding: International Conference on Damaged Ship, RINA, London.

Li, S., Kim, D.K., Benson, S., 2021. An adaptable algorithm to predict the load–shortening curves of stiffened panels in compression. Ships and Offshore Structures (Under review).

Li, S., Hu, Z., Benson, S., 2019. An analytical method to predict the buckling and collapse behaviour of plates and stiffened panels under cyclic loading. Engineering Structures, 199, 109627.

Li, S., Hu, Z., Benson, S., 2020. The sensitivity of ultimate ship hull strength to the structural component load-shortening curve. In Proceeding: 30th International Offshore and Polar Engineering Conference (ISOPE), Shanghai, China.

Li, S., Kim, D.K., Benson, S., 2021. A probabilistic approach to assess the computational uncertainty of ship hull ultimate strength. Reliability Engineering and System Safety, 213, 107688.

Smith, C.S., 1977. Influence of local compressive failure on ultimate longitudinal strength of a ship's hull. In Proceeding: International Symposium on Practical Design of Ships and others Floating Structures (PRADS), Tokyo, Japan.

Smith, C.S., Dow, R.S., 1986. Ultimate strength of a ship's hull under biaxial bending. ARE TR 86204, Admiralty Research Establishment, Dunfermline UK.

Syrigou, M., Benson, S.D., Dow, R.S., 2018. Progressive collapse assessment of intact box girders under combined bending and torsional loads. In Proceeding: 3rd International Conference on Ships and Offshore Structures (ICSOS), Gothenburg, Sweden.

Thomas, D.L., Wilson, M., Wilson, R.R., 1973. Timoshenko beam finite elements. Journal of Sound and Vibration, 31(3), 315-330.

Tatsumi, A., Ko, H., Fujikubo, M., 2020. Ultimate strength of container ships subjected to combined hogging moment and bottom local loads Part 2: An extension of Smith's method. Marine Structures, 71, 102738.

Tanaka, Y., Ogawa, H., Tatsumi, A., Fujikubo, M., 2015. Analysis method of ultimate hull girder strength under combined loads. Ships and Offshore Structures, 10(5), 587-598.

Yao T, Nikolov P. 1991. Progressive collapse analysis of a ship's hull under longitudinal bending (1st report). Journal of the Society of Naval Architects of Japan, 170, 449–461.

Yao T, Nikolov P. 1992. Progressive collapse analysis of a ship's hull under longitudinal bending (2nd report). Journal of the Society of Naval Architects of Japan, 172, 437–446.